

Exciton Band Structure in Bacterial Peripheral Light-Harvesting Complexes

Gediminas Trinkunas,^{†,‡} Oksana Zerlauskienė,[†] Vidita Urbonienė,[§] Jevgenij Chmeliov,^{†,‡} Andrew Gall,^{||} Bruno Robert,^{||} and Leonas Valkunas^{*,†,‡}

[†]Institute of Physics, Center for Physical Sciences and Technology, Savanoriu Avenue 231, LT-02300 Vilnius, Lithuania

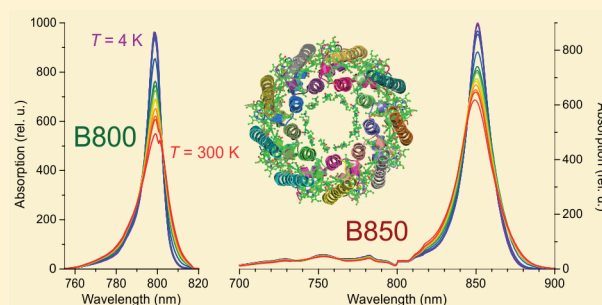
[‡]Department of Theoretical Physics, Faculty of Physics, Vilnius University, Sauletekio Avenue 9, LT-10222 Vilnius, Lithuania

[§]Department of General Physics and Spectroscopy, Faculty of Physics, Vilnius University, Sauletekio Avenue 9, LT-10222 Vilnius, Lithuania

^{||}Institute of Biology and Technology of Saclay, CNRS-URA2096, CEA-Saclay, 91191 Gif sur Yvette, France

S Supporting Information

ABSTRACT: The variability of the exciton spectra of bacteriochlorophyll molecules in light-harvesting (LH) complexes of photosynthetic bacteria ensures the excitation energy funneling trend toward the reaction center. The decisive shift of the energies is achieved due to exciton spectra formation caused by the resonance interaction between the pigments. The possibility to resolve the upper Davydov sub-band corresponding to the B850 ring and, thus, to estimate the exciton bandwidth by analyzing the temperature dependence of the steady-state absorption spectra of the LH2 complexes is demonstrated. For this purpose a self-modeling curve resolution approach was applied for analysis of the temperature dependence of the absorption spectra of LH2 complexes from the photosynthetic bacteria *Rhodobacter (Rba.) sphaeroides* and *Rhodoblastus (Rbl.) acidophilus*. Estimations of the intradimer resonance interaction values as follows directly from obtained estimations of the exciton bandwidths at room temperature give 385 and 397 cm^{-1} for the LH2 complexes from the photosynthetic bacteria *Rba. sphaeroides* and *Rhl. acidophilus*, respectively. At 4 K the corresponding couplings are slightly higher (391 and 435 cm^{-1} , respectively). The retained exciton bandwidth at physiological conditions supports the decisive role of the exciton coherence determining light absorption in bacterial light-harvesting antenna complexes.



INTRODUCTION

During the primary processes of photosynthesis antenna proteins absorb solar photons and transfer the resulting excitation energy to the reaction center, where this energy is stabilized as a chemical potential.^{1,2} Elucidation of the quaternary structure of peripheral light-harvesting complex (LH2) from the purple bacterium *Rhodoblastus (Rbl.) acidophilus*^{3,4} has provided a framework to describe these processes, both experimentally and theoretically. The LH2 complex is made of circular aggregates of dimers of trans-membrane polypeptides, which each binds three bacteriochlorophyll (Bchl) molecules in the hydrophobic phase of the membrane.^{3,4} Two of these molecules are closely packed together, and these strongly coupled Bchl molecules are responsible for the absorption band at 850 nm (the so-called B850 band), while the absorption at 800 nm (the B800 band) arises from the remaining weakly coupled Bchl molecules. As a result of the overall protein organization, the B850 and B800 bands are originated from circular arrays of strongly and weakly coupled Bchl molecules, respectively.

Due to their well-defined circular symmetry, the LH2 complexes offer a unique opportunity to confront experimental spectroscopic observations with theoretical predictions. In order to accurately describe the electronic absorption of these complexes in terms of the exciton model, the static disorder of pigment site energies as well as the dynamic disorder induced by coupling of the electronic excitations to intra- and intermolecular vibrations and phonons caused by collective vibrations of the surrounding protein should be taken into account.^{1,5–9} Exciton model parameters, in particular, the resonance intermolecular interaction between the nearest B850 pigments, are essential values for accurate description of electronic excitations of the pigment molecules arranging the ring shape structures. The resonance interaction between the nearest pigment molecules was extracted from simulation of experimental observations; however, its value varies between 300 and 420 cm^{-1} depending on whether it was determined

Received: March 1, 2012

Revised: March 25, 2012

Published: April 5, 2012

from analysis of low-temperature absorption,¹⁰ fluorescence,¹¹ or hole-burning experiments.¹² Slightly smaller values have been accessed from the quantum chemical calculations^{13,14} and using a collective electronic oscillator approach,¹⁵ which demonstrated a dominating role of protein solvation in determining the intermolecular interaction. Variability of the values of resonance interactions in the LH2 from different species and their dependencies on the approaches used for evaluation were outlined and discussed.¹⁶ The most reliable values of this parameter were defined as a measure of the exciton energy bandwidth. From the low-temperature measurements of single LH2 complexes from *Rbl. acidophilus* it was obtained that the resonance interaction typically equals 250 cm⁻¹.¹⁷ Analysis of the CD spectra of LH2 from *Rhodobacter (Rba.) sphaeroides* resulted in ~300 cm⁻¹ for the resonance interaction at room temperature, suggesting that the optical transitions into the upper excitonic states are hidden under the B800 band.^{18,19} A slightly higher value (360 cm⁻¹) was obtained from polarized fluorescence excitation at 5 K.²⁰ Two-dimensional coherent electronic spectroscopy seems also to be a relevant approach by determining values of the resonance interactions. However, first attempts by obtaining such type of spectra of the light-harvesting complexes are available for the LH3²¹ and Fenna–Matthews–Olson²² complexes so far.

All estimations of the resonance interaction values in the B850 ring were based on analysis of the experimental data obtained at fixed temperatures. However, the absorption and emission spectra of the LH2 complexes demonstrate obvious temperature dependences.^{5,7,23,24} Indeed, the B850 bands of LH2 complexes extracted from various photosynthetic bacteria shift to the blue side of the spectrum and gradually broaden with increasing temperature. The broadening of the absorption band is usually attributed to the temperature dependence of the homogeneous bandwidth. However, such attribution does not explain the band shift with temperature. According to the conventional theory developed for characterization of the electronic transitions of molecular aggregates and crystals^{1,25} or describing spectral bandwidths using Redfield theory,^{5,7,23} the exciton absorption bands should not shift with temperature. Thus, the shift of the B850 band with temperature could be attributed to conformational changes of the protein scaffold,²³ which manifest themselves in variability of the electronic transitions of the pigment molecules. To determine the possible effect of the protein conformation changes and estimate parameters of the exciton spectrum the temperature dependences of the absorption spectra of the LH2 complexes will be analyzed. For this purpose we propose a new approach of steady-state spectroscopic data mining to determine the position of the exciton absorption bands in LH2 by analyzing the temperature dependence of the absorption spectra over a large temperature range. Since the temperature dependence of the absorption spectra varies for the LH2 complexes isolated from different bacteria, we analyze the absorption spectra and determine the exciton bandwidths for the two most-studied LH2 complexes, namely, from *Rba. sphaeroides* and *Rbl. acidophilus*.

EXPERIMENTAL METHODS

The LH2 complexes from *Rba. sphaeroides* 2.4.1 and *Rbl. acidophilus* 10050 were isolated according the procedures described previously.^{5,23,26} The final composition of the LH2 samples was 20 mM Tris.Cl (pH 8.5) buffer containing 0.1% *N,N*-dimethyldodecylamine-*N*-oxide (LDAO) (w/v), 60% (v/

v) glycerol. At each temperature, the absorption spectrum was taken after a delay of 15 min, thus ensuring that the sample was fully equilibrated. Electronic absorption spectra were collected using a Varian Cary E5 double-beam scanning spectrophotometer. The temperature of the samples was maintained by a Helium bath cryostat (Maico Metriks, Tartu, Estonia). Spectra were corrected for the background absorption, as determined at each temperature using a cuvette filled with the Tris.Cl/glycerol solvent. Spectral data mining was performed using the MATLAB software package.

RESULTS

Temperature Dependence of the Absorption Spectra.

The near-infrared spectra (650–920 nm) of the LH2 complexes obtained at different temperatures are presented in Figures 1a and 2a. The B800 and B850 absorption bands of

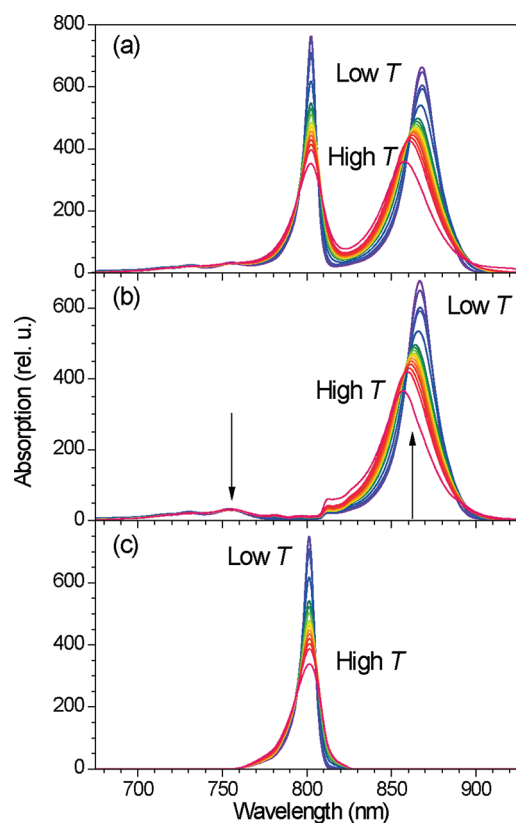


Figure 1. Absorption spectra of purified LH2 from *Rbl. acidophilus* in 60% (v/v) glycerol for the 4–300 K temperature range (a), and temperature dependence of the deconvoluted absorption spectra of B850 (b) and B800 (c) bands. Maximal absorptions at the exciton band edge states are indicated by arrows.

these complexes significantly broaden upon increasing temperature. The B800 band mainly corresponds to the optical transitions of the Bchl molecules from the sparsely organized B800 ring,^{3,4} and therefore, it shifts slightly with temperature for all species under consideration. The B850 band position is also nearly temperature independent for LH2 from *Rba. sphaeroides*; however, as temperature increases, it shifts to the blue for those isolated from *Rbl. acidophilus*. In terms of the exciton spectra, the B850 band arises mainly due to transitions to the lower Davydov sub-band of the densely packed dimerized Bchl molecules in the B850 ring.²⁷ The absorption to the upper excitonic sub-band should be very weak and

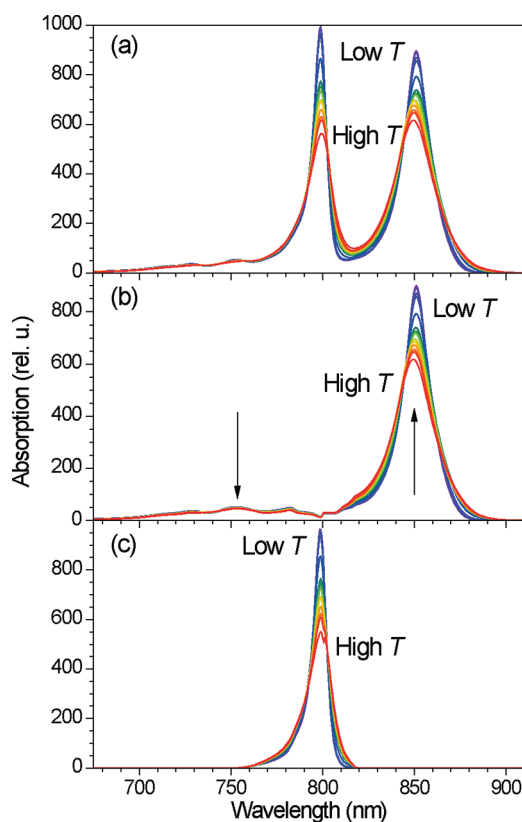


Figure 2. Absorption spectra of purified LH2 from *Rba. sphaeroides* in 60% (v/v) glycerol for the 4–250 K temperature range (a), and temperature dependence of the deconvoluted absorption spectra of B850 (b) and B800 (c) bands. Maximal absorptions at the exciton band edge states are indicated by arrows.

overlapping with the dominant transitions corresponding to the B800 ring.^{18–20,27} Knowing the position of the upper exciton sub-band of the B850 ring together with the well-defined absorption band corresponding to the transition into the lower exciton sub-band would enable us to determine the exciton bandwidth.

In order to identify the position of the upper excitonic states, the temperature dependencies of the absorption spectra presented in Figures 1a and 2a were analyzed. For this purpose we apply the self-modeling curve resolution approach²⁸ which has already been successfully used in various spectroscopic studies like protein folding recognition from CD spectra²⁹ or developing the photosynthetic activity of the reaction center from the time-resolved differential FTIR.³⁰ The idea behind this approach is based on the factorization of an initial data matrix Y of dimensions $m \times n$ (representing the absorption spectra at m wavelength points and measured for n different temperatures) as the product of two matrixes with added matrix of residuals³¹

$$Y = SD^T + E \quad (1)$$

where S is a matrix of dimensions $m \times p$ whose columns corresponding to p “pure” spectral components with amplitudes evaluated at m already chosen wavelengths; D determines the matrix of dimensions $n \times p$, where p columns represent the vectors of the weighting factors for the above-mentioned “pure” spectral components at n different temperatures. Superscript T indicates the transposed matrix, and E determines the residual matrix which is reduced to a minimal

value during the iteration process. These “pure” spectral components should be attributed to either the B800 or the B850 transition. In general, such attribution is not unique, but the task can be achieved by taking into account the fact that the amount of pigments in the B850 ring is twice that in the B800 ring, and thus, the ratio of the integral absorption of these transitions should be close to 2. Therefore, such requirement is safely added as an auxiliary constrain to eq 1.

In order to accomplish the numerical procedure of the above-formulated problem there are three main algorithms,³¹ namely, gradient descent, multiplicative update, and alternating least squares (the latter two are implemented in MATLAB). Since starting iterations with the random nonnegative matrices S and D does not produce the desired results, we use Gaussian decomposition of the LH2 absorption spectra of *Rba. sphaeroides* and *Rbl. acidophilus* using 16 and 18 sub-bands,³² respectively, as the initial values for S . The bandwidths of all these subbands and their relative amplitudes are defined from fitting experimental data. Next, we assign those Gaussian bands with maxima located around 800 nm to the B800 transition (see Figures 1c and 2c) and all others to the B850 transition. At each iteration after performing the standard algorithm steps the weighting factors in D of the “pure” spectral components belonging to B800 and B850 transitions are renormalized to ensure the ratio of the integral absorption of these transitions strictly equals 2. It appeared that the multiplicative update algorithm³¹ is the only method which showed reasonable convergence when including such constraint. Moreover, the procedure using this algorithm converged virtually to the same solution when using the initial matrixes S and D for the Gaussian decompositions of the spectra at different temperatures.³²

After removal of the components corresponding to the B800 band, the spectral properties ascribed to the excitonic transitions of the B850 ring are presented in Figures 1b and 2b for both LH2 complexes. The weak absorption on the blue side of the spectra is clearly distinguished and can be attributed to the upper excitonic sub-band. The maximal absorptions at the exciton band edges states are indicated by arrows. Pure B800 band spectra of weakly coupled Bchl molecules at different temperatures are represented in Figures 1c and 2c. Relative differences between experimental and simulated absorption spectra, calculated at each wavelength point independently, are presented in Figure 3. In the spectral region of interest the relative error does not exceed $\sim 7\%$, thus justifying application of the self-modeling curve resolution approach to extract the optical transitions corresponding to the B800 and B850 rings. The maximal positions of the excitonic transitions at different temperatures are presented in Figure 4a. All other spectroscopic data used for analysis are summarized in the Supporting Information.

Access to the Resonance Coupling from the Excitonic Absorption. The absorption spectrum of the densely packed formation of Bchl molecules in the B850 ring can be used to directly estimate the excitonic bandwidth and provide access to the resonance exciton interaction. However, this estimation is sensitive to homogeneous (fast modulation of the molecular transition energies) broadening as well as to inhomogeneous distribution of the electronic transitions of the pigment molecules due to their interaction with the protein surrounding. Both mechanisms should be taken into consideration.

The shift of both maxima of the absorption bands corresponding to the excitonic transitions in the B850 ring

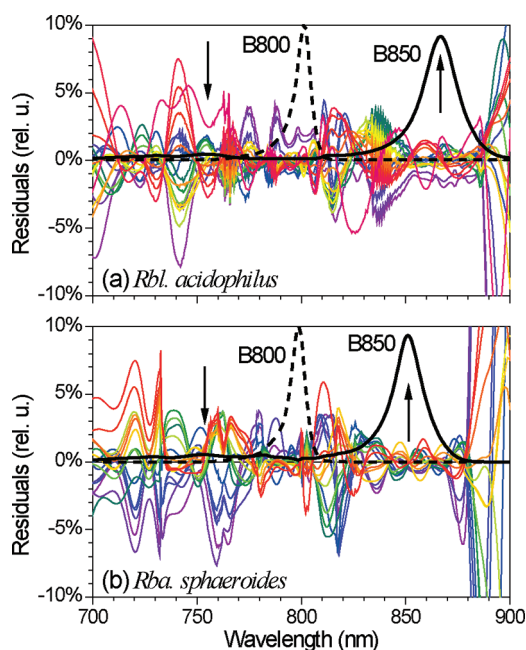


Figure 3. Relative differences between experimental and simulated absorption spectra at different temperatures for LH2 complexes from *Rbl. acidophilus* (a) and *Rba. sphaeroides* (b). For reference, the deconvoluted absorption spectra of B850 (thick solid black line) and B800 (thick dashed black line) bands at 4 K are also shown; arrows indicate the maximal absorption at the exciton band edge states. Colors correspond to spectra shown in Figures 1 and 2.

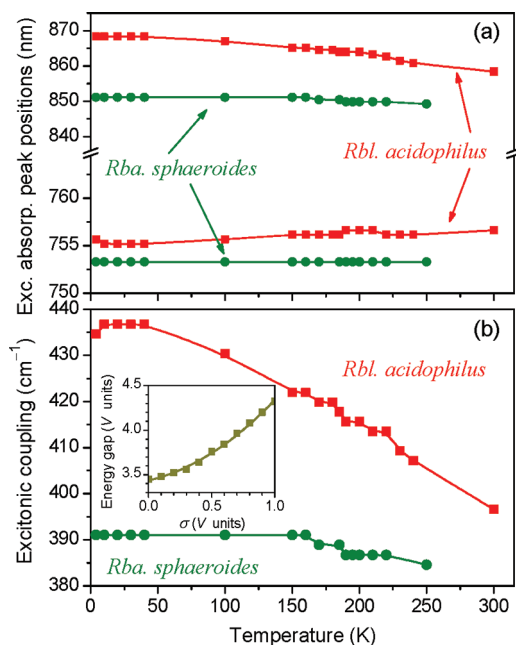


Figure 4. Positions of the absorption maxima corresponding to the excitonic transitions (a) and resonance interaction (b) at different temperatures for LH2 complexes from *Rbl. acidophilus* (squares) and *Rba. sphaeroides* (circles). Solid lines are added only to guide the eye. Inset in b shows the simulated energy gap between the absorption maxima at the edges of the exciton band and the disorder parameter σ/V . From these curves the gap scaling by resonance coupling corresponding to the optimal disorder parameter has been determined.

and therefore growth of the gap between them is sensitive to the changes of inhomogeneity or static disorder of the Bchl excitation energies. This effect can be considered in terms of a simple static disorder model of Frenkel excitons. This model consideration does not require time-consuming simulations as is the case when employing Redfield theory.^{7,23} The relevant diagonal disorder Hamiltonian of excitons in the B850 ring reads

$$H = \sum_{i=1}^N \epsilon_i |i\rangle \langle i| + \sum_{i,j=1; i \neq j}^N t_{ij} |i\rangle \langle j| \quad (4)$$

where $|i\rangle$ and $\langle i|$ represent ket and bra vectors, respectively, for the excitation localized on site i , and N is the total number of molecules in the aggregate. By considering the aggregate with cyclic boundary conditions and taking the diagonal disorder into account, the excitation energy of the i th molecule, ϵ_i , should be assumed a random variable distributed according to the normal law with the mean value ϵ^0 and with a standard deviation σ

$$P(\epsilon_i) = \frac{1}{\sqrt{2\pi}\sigma^2} \exp\left(-\frac{(\epsilon_i - \epsilon^0)^2}{2\sigma^2}\right) \quad (5)$$

Herewith we take into account all matrix elements t_{ij} denoting the resonance intermolecular interactions between molecules on sites i and j ($i \neq j$) as they can be calculated due to the known LH2 structures for *Rbl. acidophilus*.^{3,4} The exciton eigenfunctions

$$|k\rangle = \sum_{i=1}^N a_{ki} |i\rangle \quad (6)$$

and eigenenergy spectrum E_k are determined from the solution of the stationary Schrödinger equation

$$\sum_{j=1}^N \langle i|H|j\rangle a_{kj} = E_k a_{ki} \quad (7)$$

The transition intensities describing the absorption spectrum corresponding to the exciton states are then given by

$$I^k = \sum_{i,j} (\vec{\mu}_i \vec{\mu}_j) a_{ki} a_{kj} \quad (8)$$

where $\vec{\mu}_i$ is the transition dipole moment of the i th Bchl molecule.

If the disorder is neglected, the absorption of the B850 ring containing 18 Bchl molecules with all transition dipole moments oriented in the aggregate ring plane is determined by the strong transition dipole moments of the degenerate $k = \pm 1$ states at the lower excitonic sub-band and by very weak transition dipole moments of the $k = \pm 8$ states. Deviation of the orientation of these transition dipole moments out of the plane of the Bchl ring destroys the symmetry and induces a redistribution of the transition dipole moments, delivering a relevant fraction to the transitions into the neighboring exciton states on the energy scale. The relevance of such asymmetry of the dipole moments of Bchls in the B850 ring has already been reported when modeling the circular dichroism spectra of the LH2 from *Rba. sphaeroides*¹⁸ and *Rbl. acidophilus*.²⁷ Furthermore, the variations in the Bchl excitation energies also lift up the exciton state degeneracy and broaden the sharp transitions

by redistributing intensity over neighboring excitonic states (see Figure 9 in ref 23.).

Since the total excitonic bandwidth also broadens with disorder, the relevant scaling of the gap between the absorption maxima corresponding to the edges of the excitonic sub-bands can be defined only numerically. Results of such simulations on the basis of the structural data from *Rbl. acidophilus* are presented in the inset of Figure 4b, where the maximal value $V = \max\{|t_{ij}|\}$ corresponding to the intradimer dipole–dipole resonance interaction is taken as a dominating factor. Increasing the disorder enhances the deviation between the resonance interactions defined for a particular fixed disorder value (see the inset of Figure 4b). The scaling of the gap with the disorder as defined previously^{7,23} thus enables us to more precisely determine the resonance coupling values (see Table 1).

Table 1. Resonance Interactions between the Bchl Molecules of B850 Aggregate Determined from the Energy Gap between the Upper and the Lower Excitonic Absorption Maxima

	diagonal disorder ^a σ/V	scaling of the average energy gap between the exciton band edge absorptions	resonance interaction, V , cm^{-1} , at 4/300 K ^b
LH2 <i>Rba. sphaeroides</i>	0.65	3.9 V	391/385
LH2 <i>Rbl. acidophilus</i>	0.7	3.95 V	435/397

^aSee ref 7. ^bSlash mark separates the energies obtained at 4 K and room (300 K) temperature (see Figure 4b).

As follows from analysis of the simulation results, the excitonic couplings in the LH2 from different species exhibit different temperature dependences (Figure 4b). Due to the structural differences of these complexes the gaps scale differently with the magnitudes of the resonance interactions in the absence of the static disorder of the excitation energies. Their values well correlate with the full width of the exciton band, which in the absence of disorder approximately equals $2(V + V')$,²⁷ where V and V' are the resonance couplings between Bchls bound to the polypeptides of the same and neighboring dimers, respectively. These values differ more than 20% for the LH2 structure corresponding to *Rbl. acidophilus* ($V' \approx 0.77V$).^{4,13} Thus, the deviation from a simple square disorder dependence of full exciton bandwidth indicates that the low-order perturbation approach, which provides a reasonable description for the splitting between the lowest exciton levels,³³ has identifiable limitations.

DISCUSSION

The self-modeling curve resolution approach used for fitting the experimentally defined absorption spectra in a wide range of temperatures enables us to identify the positioning of the exciton transitions directly not resolvable from the spectra. This approach can be used as a selection basis between various theoretical models applied to describe the absorption spectra of diverse pigment–protein complexes. Spectral components used for decomposition of the absorption spectra of the LH2 complexes were defined by applying the sequential fitting algorithm with variable amplitudes and shapes of the components at all temperatures. The spectral components identified by means of such procedure remain to be close to Gaussian in their shapes (see Figure S1 in the Supporting

Information), and the temperature dependence of the shift and broadening of the absorption bands of the LH2 complexes is reflected in the variability of the amplitudes of the spectral components used in the decomposition procedure (Figure S2, Supporting Information).

The shift of the B850 absorption transition with temperature cannot be obtained within the framework of the conventional exciton theory, while the broadening of the band with temperature can be well described by the temperature dependence of the homogeneous bandwidth using Redfield⁷ and modified Redfield theory.²³ Recently, the Redfield equation as a second-order approach of the Quantum Master Equation was challenged as an unsuitable approximation for characterization of the excitation dynamics in photosynthesis.³⁴ Various approaches are already developed to describe an open quantum system nonperturbatively. The hierarchical equation of motion (HEOM) method is one of such methods, which was recently used for calculation of the optical line shapes of LH2 complexes.³⁵ Evidently, together with the advantages, the HEOM has also some type of disadvantages: it is numerically very expensive and scales unfavorably with the system size. Therefore, the simplified version of the HEOM method appropriate for high temperatures and using approximation for the correlation function as a finite set of exponentials was used for calculations of the absorption spectra of LH2.³⁵ Due to such limitations this type of calculation cannot be directly applied by analyzing the exciton absorption spectra for a wide temperature range. However, the B850 absorption band calculated with different correlation function parameters, which in some sense reflect the temperature dependence, evidently demonstrates that there is no shift of the band position. This can be understood as follows. Before absorbing the light the system is in its ground state, thus, the exciton states are not perturbed by interaction with the vibrational bath. Therefore, the exciton states might be considered as the reference states created by the absorption event and, thus, the conventional exciton approach should be applicable. After excitation, exciton basis starts to evolve due to the interaction with the vibrational bath, and new “effective” excitons, which are more localized (self-trapped), start to develop in time.³⁶ Such type of complexity of the exciton dynamics could be responsible for understanding the origin of different conclusions, as follows from various experimental observations using different experimental approaches.

The blue side absorption by the B850 ring defined using our deconvolution procedure of the temperature-dependent absorption spectra as shown in Figures 1b and 2b correlates with the experimentally determined spectra obtained by analyzing the kinetics of the bleaching on the red side (in the vicinity of 850 nm) depending on the excitation wavelength.³⁷ To attribute this absorption to the excitonic transitions the relevant theoretical models should be applied. In terms of exciton theory the excitonic resonance interactions V and V' are found to be temperature dependent for LH2 from *Rbl. acidophilus*, while for *Rba. sphaeroides* this dependence is virtually absent at all (Figure 4b). This observation is consistent with the extent of the shift of the absorption maximum of the B850 band upon increasing the temperature (see Figures 1a and 2a and ref 23). In seeking a relevant explanation for different temperature dependencies obtained for different species it might be important to refer to Stark spectroscopy results, which demonstrate a twice greater response to the applied electric field for the LH2 complexes from *Rbl.*

acidophilus when compared to the equivalent antenna from *Rba. sphaeroides*.³⁸

It has been recently found that the temperature dependence of the inhomogeneous distribution functions determining the excitation energy disorder has to be introduced in order to describe quantitatively the behavior of the absorption spectra.²³ The latter derives directly from the dichotomous exciton model developed by describing the spectral dynamics of a single LH2 fluorescence spectrum at room temperature.^{39,40} According to this modified exciton model, every Bchl molecule can be in two conformational states. Transitions between these conformational states modulate the excitation energies of the Bchl molecules.²³ Indeed, the differences in the temperature dependences of the resonance interaction for the LH2 complexes described above can be caused by the specific broadening and/or shift of the inhomogeneous distribution functions. Further extension of this approach can be obtained by assuming the temperature dependence of the transition energies corresponding to Bchl molecules bound to α and β helices. These values are defined by fitting absorption and CD spectra at (fixed) room temperature.^{18,19} However, the effect caused by the temperature dependence of these values can be expected if the difference between the two energies is comparable or even larger than $2(V + V')$.²⁷ Moreover, there is no physical reason to assume changes in the temperature dependence of the potential energy surface for the Bchl molecules due to the binding with the protein scaffold, as should be in the case when such assumption is valid.

Analysis of the temperature dependence of the absorption spectra of the LH2 complexes within the frame of the conventional exciton theory led to the determination of the values of the resonance interaction between the Bchl molecules from the B850 ring in LH2. For *Rba. sphaeroides*, the value of $V = 391 \text{ cm}^{-1}$ (and $V' = 301 \text{ cm}^{-1}$, as follows from the relationship $V' \approx 0.77V$)¹³ that we determined at 100 K for the resonance interaction is much higher than the $V = 300 \text{ cm}^{-1}$ determined from the CD spectra at 77 K for a B800-less mutant.¹⁸ It should be, however, noted that this mutant has an altered B850 ring with large internal voids in the protein where the Bchls corresponding to the unoccupied B800 binding site should be. It could well be that these voids introduce additional spacing between these Bchl molecules significantly reducing resonant coupling. It was well shown that the absence of B800 molecule in the complex significantly influences the electronic properties of B850.⁴¹

Trends for the temperature dependence of the Davydov splitting for the LH2 proteins from *Rbl. acidophilus* shown in this work (see Figure 4a) are qualitatively comparable with the trend defined using the fluorescence anisotropy measurements,²⁴ however, with a slight difference in the absolute values of the splitting. These discrepancies might be due to uncertainty in determining the maximum of the transition to the higher Davydov sub-band shown in Figure 4a due to possible overlap with the vibronic optical transitions. Moreover, the exciton self-trapping manifesting itself in the fluorescence^{11,20,42} can make an additional impact by attributing the fluorescence anisotropy to the Davydov components, especially in terms of the modified (dichotomous) exciton scheme. A similar discrepancy between the values in this paper obtained at 4 K ($V = 435 \text{ cm}^{-1}$, $V' = 335 \text{ cm}^{-1}$) and the ab initio molecular orbital calculations of the resonance interaction, based on the structure of the LH2 complexes from *Rbl. acidophilus* which yield a value of 320 cm^{-1} ,¹⁴ takes place.

The temperature dependence of the resonance interaction, as follows from our experimental data, could be due to the dynamics on the energy surface defined by the protein scaffold^{39,40} or a consequence of the glycerol solvent undergoing a sharp rise of its dielectric constant with temperature.^{7,43} The latter factor, however, seems to be of minor importance for the case of *Rba. sphaeroides* (see Figure 4b). It is obvious that the current resolution of the LH2 structure makes it extremely difficult to achieve a high degree of precision using ab initio calculations. Such calculations, for instance, predict a dominant effect of the Histidine ligands in the B850 ring. It was, however, experimentally shown that such effect is completely absent in the strongly coupled Bchl aggregates in the LH1 complexes.⁴⁴ It is worth noting that the values of the resonance interactions determined in this work should be considered as the upper limit of estimates since every possible temperature-dependent factor is not taken into account.

Among the novel findings in this work we show that the resonance interaction decreases with temperature for the LH2 proteins from *Rbl. acidophilus*, in contrast to the results obtained from *Rba. sphaeroides*. It is yet unclear precisely why the temperature dependence of the inhomogeneous distribution, which is a direct consequence of the dichotomous exciton model, could be at the origin of such dependence.²³ An alternative model, based on mixing of the exciton and charge transfer states,⁴⁵ could be also applied by explaining the temperature dependence of the B850 band position. However, the protein conformational changes should play the dominant role by constructing any of these models.

As demonstrated by analyzing the LH2 complexes, the temperature dependence of the absorption spectra of other pigment–protein complexes should be also considered as a good approach for studies of the exciton dynamics. Recently, the spectral variability of the major light-harvesting complexes of photosystem II and photosystem I from plants has been demonstrated by means of single molecular spectroscopy.⁴⁶ The spectral changes observed in the fluorescence spectra of single complexes at room temperature were attributed to manifestation of the dynamics on the energy surface determined by the conformational changes of the protein. Temperature dependences of the absorption and fluorescence spectra of such light-harvesting complexes could provide additional information by determining the possible role of the protein dynamics on the exciton coherence and on regulation possibilities depending on variation of the environmental conditions. Moreover, this approach, based on the relative positions of the lower and upper Davydov sub-bands of the exciton transitions, could be also used for determining the values of the resonance interactions in artificial molecular aggregates.⁴⁷

■ CONCLUSIONS

To summarize, the self-modeling curve resolution approach used by analyzing the temperature dependence of the steady-state absorption spectra of the LH2 complexes lets us resolve the upper Davydov sub-band corresponding to the B850 ring. From estimations of the gap between the upper and the lower sub-bands and by taking into account the diagonal disorder of the molecular transitions the upper bounds for the resonance interactions between Bchl molecules were estimated. Finally, the exciton bandwidth virtually persistent with temperature is attributed to the exciton coherence effect as determining the light absorption in LH2 complexes at physiological conditions.

■ ASSOCIATED CONTENT

■ Supporting Information

Explicit content of the self-modeling curve resolution procedure applied to the LH2 absorption spectra of *Rba. sphaeroides* and *Rbl. acidophilus* bacterial species measured at 16 and 18 different temperatures, respectively, in the range 4–300 K. This material is available free of charge via the Internet at <http://pubs.acs.org>.

■ AUTHOR INFORMATION

Corresponding Author

*Phone: +370-698-44472. E-mail: leonas.valkunas@ff.vu.lt.

Notes

The authors declare no competing financial interest.

■ ACKNOWLEDGMENTS

The present research was supported by the European Social Grant under the Global Grant measure, the French Agence Nationale de la Recherche (ANR) research contract ANR-07-CEXC-009 (A.G.), the European Union FP6 contract MEIF-CT-2004-00951 (A.G.), the European Union Marie Curie Host fellowship Programme contract HPMT-CT-2000-00162 (V.U.), and the Giliert programme (25543VY) from the French Ministry for Foreign and European Affairs (MAEE).

■ REFERENCES

- (1) van Amerongen, H.; Valkunas, L.; van Grondelle, R. *Photosynthetic Excitons*; World Scientific: Singapore, 2000.
- (2) Blankenship, R. E. *Molecular Mechanisms of Photosynthesis*; Blackwell Science: Oxford, 2002.
- (3) McDermott, G.; Prince, S. M.; Freer, A. A.; Hawthornthwaite-Lawless, A. M.; Papiz, M. Z.; Cogdell, R. J.; Isaacs, N. W. *Nature* **1995**, *374*, 517–521.
- (4) Papiz, M. Z.; Prince, S. M.; Howard, T.; Cogdell, R. J.; Isaacs, N. W. *J. Mol. Biol.* **2003**, *326*, 1523–1538.
- (5) Urboniene, V.; Vrublevskaja, O.; Gall, A.; Trinkunas, G.; Robert, B.; Valkunas, L. *Photosynth. Res.* **2005**, *86*, 49–59.
- (6) Vrublevskaja, O.; Urboniene, V.; Trinkunas, G.; Valkunas, L.; Gall, A.; Robert, B. *Lith. J. Phys.* **2006**, *46*, 39–46.
- (7) Urboniene, V.; Vrublevskaja, O.; Trinkunas, G.; Gall, A.; Robert, B.; Valkunas, L. *Biophys. J.* **2007**, *93*, 2188–2198.
- (8) van Grondelle, R.; Novoderezhkin, V. I. *Phys. Chem. Chem. Phys.* **2006**, *8*, 793–807.
- (9) Abramavicius, D.; Valkunas, L.; van Grondelle, R. *Phys. Chem. Chem. Phys.* **2004**, *6*, 3097–3105.
- (10) Freiberg, A.; Timpmann, K.; Ruus, R.; Woodbury, N. W. *J. Phys. Chem. B* **1999**, *103*, 10032–10041.
- (11) Freiberg, A.; Ratsep, M.; Timpmann, K.; Trinkunas, G.; Woodbury, N. W. *J. Phys. Chem. B* **2003**, *107*, 11510–11519.
- (12) Wu, H. M.; Reddy, N. R. S.; Small, G. J. *J. Phys. Chem. B* **1997**, *101*, 651–656.
- (13) Krueger, B. P.; Scholes, G. D.; Fleming, G. R. *J. Phys. Chem. B* **1998**, *102*, 5378–5386.
- (14) Scholes, G. D.; Gould, I. R.; Cogdell, R. J.; Fleming, G. R. *J. Phys. Chem. B* **1999**, *103*, 2543–2553.
- (15) Tretiak, S.; Middleton, C.; Chernyak, V.; Mukamel, S. *J. Phys. Chem. B* **2000**, *104*, 9540–9553.
- (16) Cogdell, R. J.; Gall, A.; Kohler, J. Q. *Rev. Biophys.* **2006**, *39*, 227–324.
- (17) Ketelaars, M.; van Oijen, A. M.; Matsushita, M.; Kohler, J.; Schmidt, J.; Aartsma, T. J. *Biophys. J.* **2001**, *80*, 1591–1603.
- (18) Koolhaas, M. H. C.; Frese, R. N.; Fowler, G. J. S.; Bibby, T. S.; Georgakopoulou, S.; van der Zwan, G.; Hunter, C. N.; van Grondelle, R. *Biochemistry* **1998**, *37*, 4693–4698.
- (19) Georgakopoulou, S.; Frese, R. N.; Johnson, E.; Koolhaas, C.; Cogdell, R. J.; van Grondelle, R.; van der Zwan, G. *Biophys. J.* **2002**, *82*, 2184–2197.
- (20) Timpmann, K.; Trinkunas, G.; Olsen, J. D.; Hunter, C. N.; Freiberg, A. *Chem. Phys. Lett.* **2004**, *398*, 384–388.
- (21) Zigmantas, D.; Read, E. L.; Mancal, T.; Brixner, T.; Gardiner, A. T.; Cogdell, R. J.; Fleming, G. R. *Proc. Nat. Acad. Sci. U.S.A.* **2006**, *103*, 12672–12677.
- (22) Brixner, T.; Stenger, J.; Vaswani, H. M.; Cho, M.; Blankenship, R. E.; Fleming, G. R. *Nature* **2005**, *434*, 625–628.
- (23) Zerlauskienė, O.; Trinkunas, G.; Gall, A.; Robert, B.; Urboniene, V.; Valkunas, L. *J. Phys. Chem. B* **2008**, *112*, 15883–15892.
- (24) Pajusalu, M.; Ratsep, M.; Trinkunas, G.; Freiberg, A. *ChemPhysChem* **2011**, *12*, 634–644.
- (25) Pope, M.; Swenberg, C. E. *Electronic Processes in Organic Crystals and Polymers*, 2nd ed.; Oxford University Press: New York, 1999.
- (26) Gall, A.; Robert, B. *Biochemistry* **1999**, *38*, 5185–5190.
- (27) Liuliola, V.; Valkunas, L.; van Grondelle, R. *J. Phys. Chem. B* **1997**, *101*, 7343–7349.
- (28) Lawton, W. H.; Sylvestre, E. A. *Technometrics* **1971**, *13*, 617–633.
- (29) Mendieta, J.; Diaz-Cruz, M. S.; Esteban, M.; Tauler, R. *Biophys. J.* **1998**, *74*, 2876–2888.
- (30) Blanchet, L.; Ruckebusch, C.; Mezzetti, A.; Huvenne, J. P.; de Juan, A. J. *J. Phys. Chem. B* **2009**, *113*, 6031–6040.
- (31) Berry, M. W.; Browne, M.; Langville, A. N.; Pauca, V. P.; Plemmons, R. J. *Comput. Stat. Data Anal.* **2007**, *52*, 155–173.
- (32) Urboniene, V.; Vrublevskaja, O.; Trinkunas, G.; Stakvilevicius, M.; Gall, A.; Robert, B.; Valkunas, L. *Lith. J. Phys.* **2007**, *47*, 103–108.
- (33) Jang, S.; Dempster, S. E.; Silbey, R. J. *J. Phys. Chem. B* **2001**, *105*, 6655–6665.
- (34) Ishizaki, A.; Fleming, G. R. *J. Chem. Phys.* **2009**, *130*, 234110.
- (35) Chen, L. P.; Zheng, R. H.; Shi, Q.; Yan, Y. J. *J. Chem. Phys.* **2009**, *131*, 094502.
- (36) Gelzinis, A.; Abramavicius, D.; Valkunas, L. *Phys. Rev. B* **2011**, *84*, 245430.
- (37) Gall, A.; Sogaila, E.; Gulbinas, V.; Iliaia, O.; Robert, B.; Valkunas, L. *Biochim. Biophys. Acta, Bioenerg.* **2010**, *1797*, 1465–1469.
- (38) Beekman, L. M. P.; Frese, R. N.; Fowler, G. J. S.; Picorel, R.; Cogdell, R. J.; van Stokkum, I. H. M.; Hunter, C. N.; van Grondelle, R. *J. Phys. Chem. B* **1997**, *101*, 7293–7301.
- (39) Valkunas, L.; Janusonis, J.; Rutkauskas, D.; van Grondelle, R. *J. Lumin.* **2007**, *127*, 269–275.
- (40) Janusonis, J.; Valkunas, L.; Rutkauskas, D.; van Grondelle, R. *Biophys. J.* **2008**, *94*, 1348–1358.
- (41) Gall, A.; Fowler, G. J. S.; Hunter, C. N.; Robert, B. *Biochemistry* **1997**, *36*, 16282–16287.
- (42) Trinkunas, G.; Freiberg, A. *J. Lumin.* **2006**, *119*, 105–110.
- (43) Yu, I. S. *Meas. Sci. Technol.* **1993**, *4*, 344–348.
- (44) Olsen, J. D.; Sturgis, J. N.; Westerhuis, W. H. J.; Fowler, G. J. S.; Hunter, C. N.; Robert, B. *Biochemistry* **1997**, *36*, 12625–12632.
- (45) Mancal, T.; Valkunas, L.; Fleming, G. R. *Chem. Phys. Lett.* **2006**, *432*, 301–305.
- (46) Krüger, T. P. J.; Wientjes, E.; Croce, R.; van Grondelle, R. *Proc. Nat. Acad. Sci. U.S.A.* **2011**, *108*, 13516–13521.
- (47) Hwang, I. W.; Park, M.; Ahn, T. K.; Yoon, Z. S.; Ko, D. M.; Kim, D.; Ito, F.; Ishibashi, Y.; Khan, S. R.; Nagasawa, Y.; Miyasaka, H.; Keda, C.; Takahashi, R.; Ogawa, K.; Satake, A.; Kobuke, Y. *Chem.—Eur. J.* **2005**, *11*, 3753–3761.